Natriuretic peptides block synaptic transmission by activating phosphodiesterase 2A and reducing presynaptic PKA activity

[a]Graduate School of Peking Union Medical College, Beijing 100730, China; [b]National Institute of Biological Sciences, Beijing 102206, China; [c]College of Life Sciences, Beijing Normal University, Beijing 100875, China; and [d]School of Life Sciences, Tsinghua University, Beijing 100084, China

Edited* by Paul W. Sternberg, California Institute of Technology, Pasadena, CA, and approved September 14, 2012 (received for review June 4, 2012)

postsynaptic potentials (EPSCs), whereas tetanic stimulation generates slow cholinergic responses (19).

We chose to analyze the effects of ANP application only on fast glutamatergic EPSCs with peak amplitudes over 100 pA for their stability. Because of the difficulty in obtaining stable cholinergic EPSCs with repetitive episodes of tetanic stimulation, the effect of ANP on acetylcholine release was not examined in this study. Axonal terminals were stimulated by 5-ms blue light pulses using an optical fiber with its tip directly above the IPN.

As cGMPs can also be generated by soluble GCs (sGCs) following the stimulation of nitric oxide (NO), we applied the nitric oxide synthase blocker Nω-Nitro-L-arginine methyl ester hydrochloride (L-NAME) to exclude the potential effects of NO/sGC signaling. The $GABA_A$-receptor blocker picrotoxin was also added to the bath solution to eliminate GABAergic currents. Consistent with the glutamatergic nature of the fast EPSCs (19), brief light stimulation evoked EPSCs that were resistant to the application of a mixture of two nAChR antagonists (hexamethonium and mecamylamine) (Fig. 1*D*). Strikingly, bath perfusion of ANP (100 nM) resulted in an immediate reduction in the fast EPCSs, leading to an almost complete abolishment of EPSCs in all cells tested after 10 min of ANP treatment (reduction ratio = 95%; Fig. 1

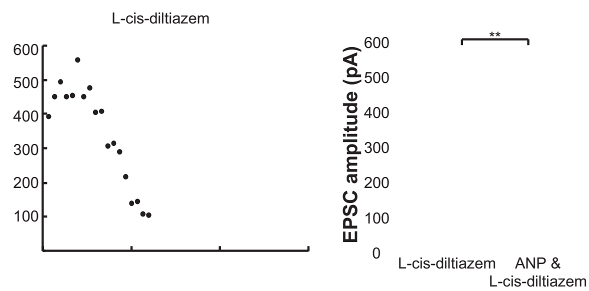

In addition to PKG and CNG channels, some PDEs are stimulated by cGMP signals. For example, PDE2A is stimulated by cGMP to hydrolyze both cGMPs and cAMPs (23). Efforts in studying PDE2A functions have been facilitated by the development of several selective PDE2A inhibitors, including 2-(3,4-dimethoxybenzyl)-7-{(1R)-1-[(1R)-1-hydroxyethyl]-4-phenylbutyl}-5-methyllimidazo[5,1-f][1,2,4]triazin-4(3H)-one (labeled as BAY 60–7550 for simplicity) and erythro-9-(2-hydroxy-3-nonyl)adenine (EHNA) (24). The fast EPSCs evoked by light stimulation were potentiated by nearly threefold from basal levels after bath application of BAY 60–7550 (1 μM) (Fig. 3 *A*–*C*). Moreover, preincubation in BAY 60–7550 largely eliminated the effect of ANP on reducing fast EPSCs. The potentiated currents were eliminated by the AMPA-type glutamate receptor antagonist CNQX (10 μM), demonstrating that they are glutamatergic in nature (Fig. 3*B*). Even in the presence of ANP, BAY 60–7550 enabled rapid reversal of EPSCs following the blockade by CNQX (Fig. 3*B*), further suggesting an antagonism of the ANP effect by BAY 60–7550. Similarly, light-evoked EPSCs were potentiated and their blockade by ANP was largely prevented by EHNA (Fig. S4 *A* and *B*), another commonly used PDE2A inhibitor (24). The efficacy of both PDE2A inhibitors on blocking ANP effects strongly suggests that PDE2A serves as the downstream transducer of cGMP signals produced by GC-A activation.

We asked whether ANP influences behaviors and whether PDE2A inhibitors can block the behavioral effects of ANP. Because the MHb is implicated in regulating behaviors related to pain and stress (25), we infused ANP into the IPN to examine its effects on nociceptive responses in behaving mice (Fig. S4*C*). In hot-plate tests, ANP infusion alone did not change the latency of behavioral response to heat (Fig. 3*D*). Challenging mice with forced swimming, which could induce stress-induced analgesia (SIA), indeed increased the response latency. In this stress-related pain behavioral paradigm, the hot-plate latency was further lengthened following ANP injection into the IPN. In addition, this lengthening of the response latency was blocked by infusion of BAY 60–7750 into the IPN before testing (Fig. 3*D*). These results thus suggest that ANP potentiates SIA by modulating the physiological properties of the MHb–IPN pathway. In addition, the behavioral effect of ANP requires the activity of PDE2A.

An earlier study reports PDE2A expression in the MHb and IPN (26), but it was unclear whether PDE2A is specifically expressed in the axonal terminals of MHb neurons. We observed PDE2A immunoreactivity in the somata of MHb neurons (Fig. S5 *A* and *B*). In the IPN, PDE2A was expressed only in the synaptic terminals (Fig. 4 *A* and *B* and Fig. S5*C*). PDE2A expression was restricted to ChR2-EYFP+ axonal terminals in the dorsal and central IPN subnuclei (Fig. 4*B* and Fig. S5*C*), which are targeted by the axonal projection from MHb cholinergic neurons (18, 19).

Because both cGMPs and cAMPs are the substrates of PDE2A (23), we asked whether ANP application could reduce presynaptic cAMP levels via PDE2A activity. ELISA measurements revealed that ANP significantly reduced the cAMP concentrations in the IPN to less than half of basal levels, and this reduction was prevented by blocking PDE2A activity with BAY 60–7550 pretreatment (Fig. 4*C*). BAY 60–7750 alone increased cAMP levels by over fourfold, supporting the role of PDE2A in suppressing constitutive cAMP accumulation and thus transmitter release (Fig. 3). Moreover, ANP substantially reduced cAMP levels following the stimulation of adenylyl cyclase by forskolin, and this reduction was blocked by BAY 60–7550 pretreatment (Fig. 4*D*).

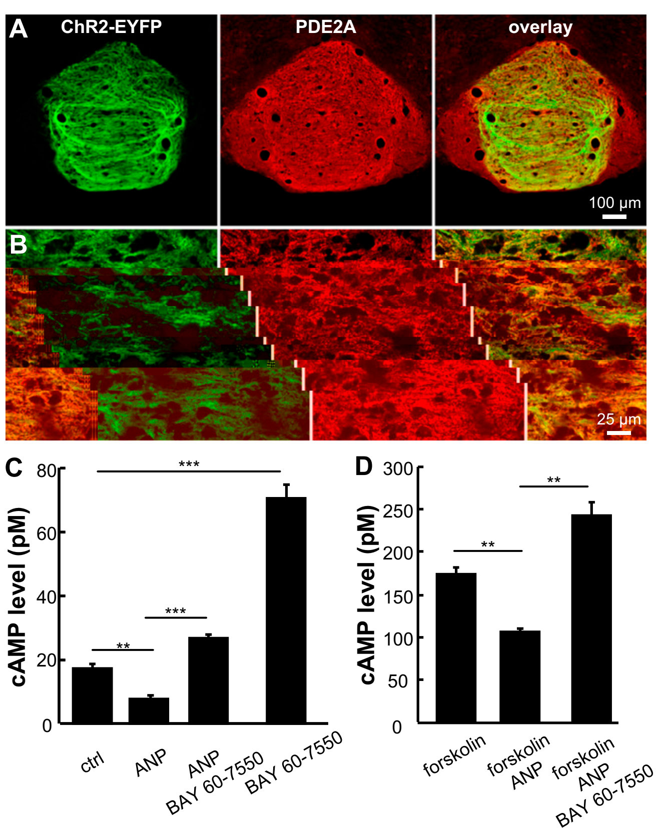

. 4. PDE2A is richly expressed in the axonal terminals of MHb neurons and negatively regulates cAMP levels in the IPN. (*A*) Confocal image of a coronal section from a ChAT-ChR2-EYFP mouse showing the expression of PDE2A (red) in ChR2-EYFP+ terminals (green) in the IPN. (*B*) High-magnification views show that essentially all ChR2-EYFP-labeled axonal terminals (green) are immunopositive for PDE2A (red) in the IPN. (*C* and *D*) ANP substantially reduces basal (*C*) and forskolin (25 μM)-evoked (*D*) cAMP levels in the IPN, and this reduction is reversed by blocking PDE2A with BAY 60–7750 (10 μM). Application of the PDE2A blocker alone increases cAMP levels (***P* < 0.01; ****P* < 0.001; within-group *t* tests; *n* = 4 separate readings for each group). (*C* and *D*) Error bars indicate SEM.

These biochemical measurements thus demonstrate that ANP can activate PDE2A to efficiently reduce cAMP levels in the IPN.

Eff f ANP I L P D P K A A . We investigated how PDE2A shapes downstream signals to block glutamate transmission. Both the cAMP-sensitive protein kinase A (PKA) and the exchange protein activated by cAMP (Epac) have been implicated in modulating neurotransmitter release in various brain areas (27). By applying the membrane-permeable PKA activator 6-BNZ-cAMP, we tested whether direct PKA activation could rescue fast EPSCs following their blockade by ANP. For all cells tested (*n* = 6 cells), EPSCs were blocked by ANP and then fully recovered after bath application of 6-BNZ-cAMP (Fig. 5 *A*–*C*). In current-clamp mode, 6-BNZ-cAMP reversed the ANP blockade and enabled IPN neurons to be depolarized and fire action potentials in response to light stimulation (Fig. S6*A*). In contrast to the effectiveness of the PKA activator 6-BNZ-cAMP, application of the selective Epac activator 8-CPT-2Me-cAMP failed to reverse the ANP blockade (Fig. S6 *B* and *C*).

We used PKA inhibitors to further examine the role of basal PKA activity in regulating glutamate release. EPSCs were reduced by ~70% after bath perfusion of a mixture of PKA inhibitors (H89 and Rp-8-Br-cAMP; Fig. 5 *D* and *E*). The residual current may be explained by an insufficient ability of PKA inhibitors to fully block intracellular PKA activity after permeating the cell membrane. Additional analyses show that PKA inhibitors did not affect the frequency or amplitude of spontaneous EPSCs in IPN neurons (Fig. S6 *D*–*G*), indicating that the substantial suppression of EPSCs by PKA inhibitors results from changes in presynaptic terminals but not in postsynaptic neurons.

D .

Since their original discovery in 1980s (7–9, 13), natriuretic peptides and their receptors have been found to be richly expressed in several brain areas (12, 13, 17). However, their physiological functions as well as the underlying signaling mechanisms in the brain remain poorly understood. In this study, we find that ANP application in the IPN abolishes synaptic release of glutamate from habenular axonal terminals. Furthermore, we show that the ANP effects are mediated by PDE2A activity, which in turn depletes cAMP and thus eliminates basal PKA activity. Our data demonstrate a strong effect of presynaptic inhibition by natriuretic peptides and delineate a signaling pathway through which cGMP signals block neurotransmitter release by negatively coupling to cAMP pathways (Fig. 5*F*).

ANP or BNP produces an almost complete blockade of glutamate release by MHb neurons, indicating that they are very strong presynaptic inhibitors. The inhibitory effects of natriuretic peptides appear much weaker in other areas of the nervous system. In the C-fibers from the dorsal root ganglia, BNP reduces glutamatergic EPSCs by ~30% (28). ANP weakens EPSCs by 46% for the connection between osmoreceptor neurons in the organum vasculosum laminae terminalis and the magnocellular neurosecretory cells in the supraoptic nucleus (29). In the retina, BNP functions as a postsynaptic modulator and produces a roughly 40% suppression of $GABA_A$-receptor–mediated inhibitory currents in bipolar cells (30).

Our results differ from previous studies that highlight a pivotal role of PKG in mediating the effect of natriuretic peptides in the dorsal root ganglia and the retina (28, 30). For the connection between the MHb and IPN, PKG blockers do not disrupt the shut-off effect of ANP, and PKG activators do not change EPSCs. In contrast, ANP is completely antagonized by PDE2A blockers. Biochemical and imaging studies of culture cells have shown that PDE2A is capable of efficiently depleting cAMPs following cGMP stimulation (23, 31). Our biochemical assays show that ANP reduces cAMP levels in the IPN area of brain slices and that this reduction is fully blocked by applying PDE2A inhibitors. In addition, presynaptic inhibition of glutamate release by ANP is reversed by a PKA activator, and the ANP effect is largely mimicked by PKA inhibitors. These results indicate that ANP blocks neurotransmission by depleting presynaptic cAMP concentrations. Interestingly, the signal transduction cascade in the axonal terminals of MHb neurons is reminiscent of that in nonneuronal cells in the periphery. In both adrenal glomerulosa cells and cardiac myocytes, ANP activates its receptors to produce cGMPs, which in turn stimulate PDE2A to reduce intracellular cAMP levels (32–34). Therefore, negative crosstalk between cGMP and cAMP cascades might be one of the conserved mechanisms underlying natriuretic peptide action both inside and outside the nervous system. PDE2A has been thought to serve simply as a cGMP scavenger in olfactory CO_2 neurons (35, 36). Our physiological recordings suggest that PDE2A performs the important function of regulating neurotransmitter release by negatively linking cGMP signals to the cAMP pathway.

The MHb–IPN pathway is believed to be related to anxiety and nicotine addiction (14, 15). Our behavioral tests indicate that ANP enhances stress-induced analgesia in a PDE2A-dependent manner. This finding is consistent with the facts that the MHb receives input from forebrain septal areas that are involved in stress-related behaviors and that MHb neurons express opiate receptors (18, 25). The exact sources of ANP or BNP in the IPN remain unclear. An early study indicated that ANP may be expressed by MHb neurons (11), suggesting the possibility of presynaptic inhibition by autocrine signaling of ANP. Alternatively, ANP might be transported to the IPN following their production in the heart. Although the exact behavioral context for ANP release into the IPN remains unclear, our results suggest that the ANP signaling can regulate animal behaviors by modulating neurotransmission in the habenulo-interpeduncular pathway. Furthermore, the powerful and selective PDE2A inhibitors have contributed to the elucidation of PDE2A functions but have

(200 μM; Sigma), 8-CPT-2Me-cAMP (50 μM; Tocris), 8-pCPT-cGMP (100 μM; Sigma), CNQX or DNQX (10 μM; Sigma), L-*cis*-Diltiazem (10 μM; Biomol), EHNA (90 μM; Sigma), H89 (30 μM; Sigma) and Rp-8-Br-cAMP (170 μM; Biolog), KT5823 (2 μM; Biomol), L-NAME (100 μM; Sigma), picrotoxin (50 μM; Sigma), Rp-8-pCPT-cGMP (10 μM; Biomol), TTX (1 μM; Sigma), and a mixture of hexamethonium-Cl (50 μM; Sigma) and mecamylamine (5 μM; Sigma). The effectiveness of Rp-8-pCPT-cGMP, KT5823, 8-Br-cGMP, and L-*cis*-Diltiazem has been confirmed by recent studies in our group (6, 35). AMPA (17.5 μM; Sigma) and acetylcholine (1 mM; Sigma) were pressure-ejected using an eight-channel drug delivery system (MPS-1, Inbio Life Science Instrument), with the tip of the drug delivery pipette located ∼500 μm away from the recording site. Picrotoxin and L-NAME was added to the recording solution to block $GABA_A$-receptor–mediated transmission and the effects mediated by sGCs. At least 5 min of baseline was collected from each cell.

M f GMP AMP L. Brain slices (250 μm thick) containing the IPN were prepared from ChAT-ChR2-EYPF mice and recovered in oxygenated aCSF for 40 min at 34 °C. The tissues were then incubated with the following drugs for 20 min: ANP (100 nM), BAY60-7550 (10 μM), forskolin (25 μM), and 3-isobutyl-1-methylxanthine (IBMX; 1 mM). The IPN area was dissected out under the visual guidance of fluorescent microscopy and lysed with 0.1 mM HCl for 5 min. Tissues were further disrupted with an ultrasound probe for 10 min and centrifuged (14,000 × *g*) at 4 °C for 10 min. The concentrations of cGMP or cAMP in the supernatant were measured with ELISA kits (NewEast Biosciences Inc., catalog no. 80101 or 80202).

H C f I. Cells were filled with Neurobiotin (0.25%; Vector Laboratories) in the intrapipette recording solution. Brain slices after recordings were fixed with 4% (wt/vol) paraformaldehyde in 0.1 M PBS, and neurons were stained with Cy3-conjugated streptavidin (1:500; 2 h) in 0.1 M PBS with 0.3% Triton-X. For PDE2A immunostaining, adult mouse brain was fixed and cryoprotected in 30% (wt/vol) sucrose. Frozen tissue was sectioned coronally at 40 μm thickness with a microtome (Leica CM 1900). After rinsing with 0.3% Triton-X in 0.1 M PBS and blocking with 2% (wt/vol) normal bovine serum for 1 h, sections were incubated with a rabbit anti-PDE2A antibody in the blocking solutions (1:200, 12 h in 4 °C; FabGennix Inc., PD2A-101AP). After rinsing, sections were then incubated with Cy3-conjugated goat anti-rabbit antibody for 2 h at room temperature (1:500; Jackson ImmunoResearch). Fluorescent images were acquired by a Carl Zeiss 510 confocal microscope.

B A. Mice were anesthetized with pentobarbital (80 mg/kg i.p.), and a guide cannula was implanted with its tip 0.5 mm above the IPN. One week later, mice were first exposed to forced swimming in a glass cylinder partially filled with 22–25 °C water for 8 min. After a 2-d recovery, drug or aCSF control (1 μL) was infused into the IPN through an internal cannula for 10 min (RWD202 Syringe Pump, RWD Life Science). Seven minutes later, mice were placed on a hot plate (Taimeng Technology), the temperature of which was set at 54.5 ± 0.5 °C. We assessed the baseline nociception response by measuring the latency to first hindpaw licking, tapping, or four-paw jumping. To test the effect of SIA the next day, all mice were injected with aCSF or drugs into the IPN and immediately immersed in cold water (4 °C) for 2 min. To measure the effect of BAY 60–7550 on ANP (10 μM)-induced SIA enhancement, we first injected 0.5 μL of BAY 60–7550 (25 μM) and then a 0.5-μL mixture of ANP (20 μM) and BAY 60–7550 (25 μM). Mice were then dried with paper towels and rested for 3 min before the hot-plate test.

1. We thank G. Feng (Massachusetts Institute of Technology) for ChAT-ChR2-EYFP mice and Z. Liu and C. Qin (National Institute of Biological Sciences) for help with behavioral assays. M.L. is supported by China Ministry of Science and Technology 973 Grant 2010CB833902.

1. Miller RJ (1998) Presynaptic receptors. *Annu Rev Pharmacol Toxicol* 38:201–227.
2. Lucas KA, et al. (2000) Guanylyl cyclases and signaling by cyclic GMP. *Pharmacol Rev* 52(3):375–414.
3. Potter LR, Yoder AR, Flora DR, Antos LK, Dickey DM (2009) Natriuretic peptides: Their structures, receptors, physiologic functions and therapeutic applications. *Handb Exp Pharmacol* 191:341–366.
4. Reaume CJ, Sokolowski MB (2009) cGMP-dependent protein kinase as a modifier of behaviour. *Handb Exp Pharmacol* 191:423–443.
5. Tsunozaki M, Chalasani SH, Bargmann CI (2008) A behavioral switch: cGMP and PKC signaling in olfactory neurons reverses odor preference in C. elegans. *Neuron* 59(6):959–971.
6. Gong R, et al. (2011) Role for the membrane receptor guanylyl cyclase-C in attention deficiency and hyperactive behavior. *Science* 333(6049):1642–1646.
7. de Bold AJ (1985) Atrial natriuretic factor: A hormone produced by the heart. *Science* 230(4727):767–770.
8. Lang RE, et al. (1985) Atrial natriuretic factor: A circulating hormone stimulated by volume loading. *Nature* 314(6008):264–266.
9. Chinkers M, et al. (1989) A membrane form of guanylate cyclase is an atrial natriuretic peptide receptor. *Nature* 338(6210):78–83.
10. Saper CB, et al. (1985) Atriopeptin-immunoreactive neurons in the brain: Presence in cardiovascular regulatory areas. *Science* 227(4690):1047–1049.
11. Skofitsch G, Jacobowitz DM, Eskay RL, Zamir N (1985) Distribution of atrial natriuretic factor-like immunoreactive neurons in the rat brain. *Neuroscience* 16(4):917–948.
12. Quirion R, Dalpé M, Dam TV (1986) Characterization and distribution of receptors for the atrial natriuretic peptides in mammalian brain. *Proc Natl Acad Sci USA* 83(1):174–178.
13. Gibson TR, Wildey GM, Manaker S, Glembotski CC (1986) Autoradiographic localization and characterization of atrial natriuretic peptide binding sites in the rat central nervous system and adrenal gland. *J Neurosci* 6(7):2004–2011.
14. Fowler CD, Lu Q, Johnson PM, Marks MJ, Kenny PJ (2011) Habenular α5 nicotinic receptor subunit signalling controls nicotine intake. *Nature* 471(7340):597–601.
15. Agetsuma M, et al. (2010) The habenula is crucial for experience-dependent modification of fear responses in zebrafish. *Nat Neurosci* 13(11):1354–1356.
16. Hikosaka O (2010) The habenula: From stress evasion to value-based decision-making. *Nat Rev Neurosci* 11(7):503–513.
17. Herman JP, Dolgas CM, Rucker D, Langub MC, Jr. (1996) Localization of natriuretic peptide-activated guanylate cyclase mRNAs in the rat brain. *J Comp Neurol* 369(2):165–187.
18. Qin C, Luo M (2009) Neurochemical phenotypes of the afferent and efferent projections of the mouse medial habenula. *Neuroscience* 161(3):827–837.
19. Ren J, et al. (2011) Habenula "cholinergic" neurons co-release glutamate and acetylcholine and activate postsynaptic neurons via distinct transmission modes. *Neuron* 69(3):445–452.
20. Suga S, et al. (1992) Receptor selectivity of natriuretic peptide family, atrial natriuretic peptide, brain natriuretic peptide, and C-type natriuretic peptide. *Endocrinology* 130 (1):229–239.
21. Standaert DG, Cechetto DF, Needleman P, Saper CB (1987) Inhibition of the firing of vasopressin neurons by atriopeptin. *Nature* 329(6135):151–153.
22. White RE, et al. (1993) Potassium channel stimulation by natriuretic peptides through cGMP-dependent dephosphorylation. *Nature* 361(6409):263–266.
23. Martins TJ, Mumby MC, Beavo JA (1982) Purification and characterization of a cyclic GMP-stimulated cyclic nucleotide phosphodiesterase from bovine tissues. *J Biol Chem* 257(4):1973–1979.
24. Boess FG, et al. (2004) Inhibition of phosphodiesterase 2 increases neuronal cGMP, synaptic plasticity and memory performance. *Neuropharmacology* 47(7):1081–1092.
25. Herkenham M, Pert CB (1980) In vitro autoradiography of opiate receptors in rat brain suggests loci of "opiatergic" pathways. *Proc Natl Acad Sci USA* 77(9):5532–5536.
26. Juilfs DM, Soderling S, Burns F, Beavo JA (1999) Cyclic GMP as substrate and regulator of cyclic nucleotide phosphodiesterases (PDEs). *Rev Physiol Biochem Pharmacol* 135:67–104.
27. Seino S, Shibasaki T (2005) PKA-dependent and PKA-independent pathways for cAMP-regulated exocytosis. *Physiol Rev* 85(4):1303–1342.
28. Zhang FX, et al. (2010) Inhibition of inflammatory pain by activating B-type natriuretic peptide signal pathway in nociceptive sensory neurons. *J Neurosci* 30(32): 10927–10938.
29. Richard D, Bourque CW (1996) Atrial natriuretic peptide modulates synaptic transmission from osmoreceptor afferents to the supraoptic nucleus. *J Neurosci* 16 (23):7526–7532.
30. Yu YC, Cao LH, Yang XL (2006) Modulation by brain natriuretic peptide of GABA receptors on rat retinal ON-type bipolar cells. *J Neurosci* 26(2):696–707.
31. Nikolaev VO, Gambaryan S, Engelhardt S, Walter U, Lohse MJ (2005) Real-time monitoring of the PDE2 activity of live cells: Hormone-stimulated cAMP hydrolysis is faster than hormone-stimulated cAMP synthesis. *J Biol Chem* 280(3):1716–1719.
32. MacFarland RT, Zelus BD, Beavo JA (1991) High concentrations of a cGMP-stimulated phosphodiesterase mediate ANP-induced decreases in cAMP and steroidogenesis in adrenal glomerulosa cells. *J Biol Chem* 266(1):136–142.
33. Méry PF, Pavoine C, Pecker F, Fischmeister R (1995) Erythro-9-(2-hydroxy-3-nonyl)adenine inhibits cyclic GMP-stimulated phosphodiesterase in isolated cardiac myocytes. *Mol Pharmacol* 48(1):121–130.
34. Vandecasteele G, Verde I, Rücker-Martin C, Donzeau-Gouge P, Fischmeister R (2001) Cyclic GMP regulation of the L-type Ca(2+) channel current in human atrial myocytes. *J Physiol* 533(Pt 2):329–340.
35. Hu J, et al. (2007) Detection of near-atmospheric concentrations of CO2 by an olfactory subsystem in the mouse. *Science* 317(5840):953–957.
36. Luo M, Sun L, Hu J (2009) Neural detection of gases—carbon dioxide, oxygen—in vertebrates and invertebrates. *Curr Opin Neurobiol* 19(4):354–361.
37. Masood A, Nadeem A, Mustafa SJ, O'Donnell JM (2008) Reversal of oxidative stress-induced anxiety by inhibition of phosphodiesterase-2 in mice. *J Pharmacol Exp Ther* 326(2):369–379.
38. Menniti FS, Faraci WS, Schmidt CJ (2006) Phosphodiesterases in the CNS: Targets for drug development. *Nat Rev Drug Discov* 5(8):660–670.
39. Greengard P, Jen J, Nairn AC, Stevens CF (1991) Enhancement of the glutamate response by cAMP-dependent protein kinase in hippocampal neurons. *Science* 253 (5024):1135–1138.
40. Salin PA, Malenka RC, Nicoll RA (1996) Cyclic AMP mediates a presynaptic form of LTP at cerebellar parallel fiber synapses. *Neuron* 16(4):797–803.
41. Sakaba T, Neher E (2003) Direct modulation of synaptic vesicle priming by GABA(B) receptor activation at a glutamatergic synapse. *Nature* 424(6950):775–778.